

## A Simple Method to the Fabrication of Rectangular $\text{Co}_3\text{O}_4$ Nanosheets

Xiaomin Ni,<sup>1</sup> Jimei Song,<sup>1</sup> Dongguo Li,<sup>1</sup> Yongfeng Zhang,<sup>2</sup> and Huagui Zheng<sup>\*1</sup>

<sup>1</sup>Department of Chemistry, University of Science and Technology of China,  
Hefei, Anhui, 230026, P. R. China

<sup>2</sup>State Key Lab of Fire Science, University of Science and Technology of China,  
Hefei, Anhui, 230026, P. R. China

(Received October 2, 2006; CL-061154; E-mail: hgzheng@ustc.edu.cn)

Rectangular  $\text{Co}_3\text{O}_4$  nanosheets with the thickness of about 50–100 nm were fabricated by calcining the isomorphological  $\text{Co}(\text{CO}_3)_{0.35}\text{Cl}_{0.20}(\text{OH})_{1.10}$  precursor, which were produced via the reaction of  $\text{CoCl}_2$  and  $\text{CO}(\text{NH}_2)_2$  in the presence of PEG (polyethylene glycol)-10000. Thus-prepared  $\text{Co}_3\text{O}_4$  sheets exhibited high efficiency for the growth of carbon nanotubes in pyrolyzing ethanol.

Spinel  $\text{Co}_3\text{O}_4$  is an important transition-metal oxide whose applications span over a wide range of fields, including magnetic p-type semiconductor, solid-state sensors, ceramic pigments, intercalation compounds for energy storage, rotatable magnets, heterogeneous catalysts, and electrochromic devices.<sup>1–7</sup> Some of its uses today and future would benefit from the materials designed down to nanosize and novel morphology. For example, mesoporous  $\text{Co}_3\text{O}_4$  exhibited a Brunauer–Emmett–Teller ( $\text{N}_2$ ) surface area of  $212\text{ m}^2/\text{g}$  and a high specific electrochemical capacitance of  $401\text{ F/g}$ .<sup>8</sup> One-dimensional arrays of  $\text{Co}_3\text{O}_4$  nanoparticles delivered a discharge capacity of  $1150\text{ mAh/g}$  and at  $1\text{ Li}^+/5\text{ h}$ , while the capacity of bulk counterparts was only  $850\text{ mAh/g}$ .<sup>9</sup>  $\text{Co}_3\text{O}_4$  nanotubes exhibited superior gas-sensing capabilities toward  $\text{H}_2$  and alcohol than the  $\text{Co}_3\text{O}_4$  nanoparticles.<sup>10</sup> Up to date, a large variety of  $\text{Co}_3\text{O}_4$  nanocrystals with different shapes have been fabricated, such as nanofibers, nanocubes, hollow spheres, and porous nanotubes with respect to morphology-dependent properties and applications.<sup>11–14</sup> In this manuscript, we reported the preparation of a new type of sheetlike  $\text{Co}_3\text{O}_4$  nanocrystals. The synthetic process involved two steps, in which  $\text{Co}(\text{CO}_3)_{0.35}\text{Cl}_{0.20}(\text{OH})_{1.10}$  nanosheets were prepared first by hydrothermal treatment of urea and cobalt chloride with the assistance of PEG-10000, then the precursor was calcined at  $550^\circ\text{C}$  for 2 h. Morphology details and catalytic properties of thus-prepared  $\text{Co}_3\text{O}_4$  nanosheets for the growth of carbon nanotubes were investigated.

All chemicals were of analytical grade and used without purification. A typical experiment was as following: 0.2 g of PEG-10000 (polyethylene glycol with molecular weight of 10000) was dissolved into 35 mL of aqueous solution containing 0.01 M  $\text{CoCl}_2 \cdot 6\text{H}_2\text{O}$  and 0.04 M urea under magnetic stirring. The mixture was then transferred into a 40-mL autoclave, sealed, and maintained at  $120^\circ\text{C}$  for 24 h. After the heat treatment was over, the resulting pink-colored precipitate was collected, rinsed with distilled water and ethanol for several times, and finally vacuum dried at  $50^\circ\text{C}$  for 4 h. For the preparation of  $\text{Co}_3\text{O}_4$ , part of the powder was heated in air condition at  $550^\circ\text{C}$  for 2 h, which resulted in the final black product. For the synthesis of carbon nanotubes, 40 mg of  $\text{Co}_3\text{O}_4$  powder was added into a 20-mL stainless autoclave containing 12 mL of ethanol. The

clave was then sealed, heated at a rate of  $5^\circ\text{C}/\text{min}$  to  $550^\circ\text{C}$ , and kept at the temperature for 12 h. After theclave was cooled to room temperature on standing, the black precipitate was collected and immersed in dilute  $\text{HNO}_3$  solution under stirring for 12 h. The products were centrifuged, rinsed with distilled water and absolute ethanol, and finally vacuum dried at  $50^\circ\text{C}$  for 2 h.

X-ray diffraction (XRD) pattern of the sample was recorded on a Philips X'pert diffractometer with  $\text{Cu K}\alpha$  radiation ( $\lambda = 1.5418\text{ \AA}$ ). The morphology and structure of the sample were studied with a field emission scanning electron microscope (FE-SEM, JEOL JSM-6300F) and a transmission electron microscope (TEM, Hitachi H-800) with an accelerating voltage of 200 kV.

Figures 1a and 1b gave the XRD patterns of the precursor and the final product, which could be indexed as  $\text{Co}(\text{CO}_3)_{0.35}\text{Cl}_{0.20}(\text{OH})_{1.10}$  (JCPDS: 38-0547) and  $\text{Co}_3\text{O}_4$  (JCPDS: 09-0418), respectively. No other impurities were observed, indicating that two pure samples were obtained by the present procedures.

Morphologies of the two samples were studied by SEM and TEM. Figure 2a showed that the precursor consisted of rectangular sheets with the side length of about 5–10  $\mu\text{m}$ , in which smaller sheets superposed on the bottom big one. Figure 2b exhibited a panoramic image of the calcined product, which basically inherited the size and morphology of the precursor. Magnified images of Figures 2c and 2d revealed that the  $\text{Co}_3\text{O}_4$  sheets with the thickness of about 50–100 nm were apparently porous, which were made up of interconnected spherical nanocrystals with the size of about 20 nm. Formation of the porous sheets was possibly ascribed to the thermal decomposition that resulted in a lot of nanoparticles and gaps/pores between the particles simultaneously. However, the removal of the superfluous molecules did

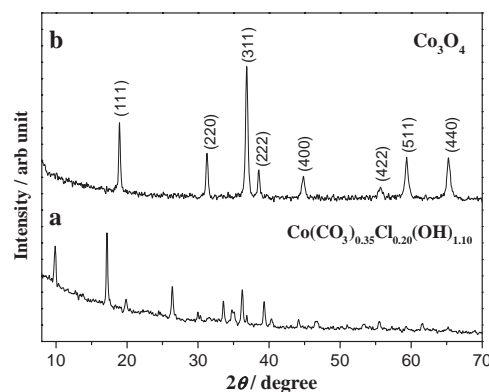


**Figure 1.** XRD patterns of as-prepared  $\text{Co}(\text{CO}_3)_{0.35}\text{Cl}_{0.20}(\text{OH})_{1.10}$  precursor (a) and  $\text{Co}_3\text{O}_4$  sheets (b).

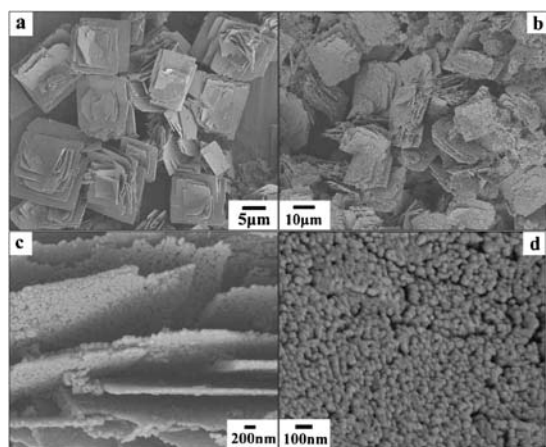


**Figure 2.** Morphological SEM images of the precursor (a) and the calcined product of  $\text{Co}_3\text{O}_4$  (b). (c) and (d) were the corresponding magnified images of the  $\text{Co}_3\text{O}_4$  sheets.

not damage the former geometrical shape, which was possibly due to the nanocontact between each particle that stabilized the sheetlike morphology mechanically against collapse or fracture.<sup>15</sup>

The polymer of PEG-10000 played an important role for the formation of the sheetlike precursor. Control experiments demonstrated that without PEG-10000 only flowery crystallites with the radially bunched nanorods were obtained for the usual growth tendency of  $\text{Co}(\text{CO}_3)_{0.35}\text{Cl}_{0.20}(\text{OH})_{1.10}$ .<sup>16</sup> It was considered that PEG-10000 changed the growth orientation of the precursor into two-dimensional crystals. During the reaction process, PEG-10000 may selectively absorb on some crystal faces and inhibited their development, which finally resulted in sheetlike morphology. When calcined in air condition, the precursors gradually decomposed, accompanied by partial oxidation of  $\text{Co}^{\text{II}}$  to  $\text{Co}^{\text{III}}$ .

Thus-prepared  $\text{Co}_3\text{O}_4$  nanosheets show high efficiency for the growth of carbon nanotubes in pyrolyzing ethanol. Figure 3a gave a typical SEM image of the resulting carbon par-

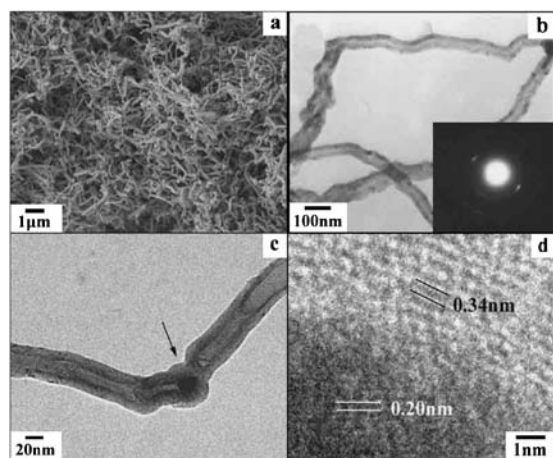


**Figure 3.** SEM images of the resulting carbon nanotubes (a) and TEM image of the carbon nanotubes (b), inset was the corresponding SAED pattern. (c) and (d) were a typical nanotube containing catalyst particle and the corresponding HRTEM image.

ticles, in which the yield of carbon nanotubes was above 95% by SEM observations, which suggests that the selectivity for carbon nanotubes was above 95% while sheetlike product was not found. The nanotubes had the inner diameter of about 40 nm and the wall thickness of about 20 nm. The corresponding selected area electron diffraction (SAED) pattern was taken on the middle of the tubes, which was characteristic of carbon nanotubes. Figure 3c presented a typical nanotube with a catalyst particle enveloped in it. Figure 3d was the corresponding HRTEM image, revealing that the carbon nanotubes were multiwalled, and the inner catalyst particle was due to the metallic cobalt. Formation of the nanotubes could be ascribed to the metallic cobalt reduced from  $\text{Co}_3\text{O}_4$ , in which ethanol played as carbon source and reducing agent.<sup>17</sup> Similar catalysis for the production of carbon nanotubes of transitional-metal oxides was also found in the cases of  $\text{NiO}$  and  $\text{Co}_2\text{O}_3$ .<sup>17,18</sup> Further research on the real catalytic mechanism is underway.

In summary, we reported the synthesis of sheetlike  $\text{Co}_3\text{O}_4$  nanocrystals by a simple two-step method. The process involved the calcination of isomorphological precursor, which were first prepared by hydrothermally treating the mixture of urea and cobalt chloride in the presence of PEG-10000. Thus-prepared  $\text{Co}_3\text{O}_4$  nanosheets exhibited high efficiency for the production of carbon nanotubes in pyrolyzing ethanol, which provided a simple method for large scale synthesis of carbon nanotubes from cheap and harmless reagents. More usages are expected to be found for the special  $\text{Co}_3\text{O}_4$  nanosheets.

## References

- 1 M. Ocana, A. R. Gozalez-Elipe, *Colloids Surf. A* **1999**, 157, 315.
- 2 T. Sugimoto, E. Matijevic, *J. Inorg. Nucl. Chem.* **1979**, 41, 165.
- 3 D. Barreca, C. Massignan, S. Daolio, M. Fabrizio, C. Piccirillo, L. Armelao, E. Tondello, *Chem. Mater.* **2001**, 13, 588.
- 4 E. Matijevic, *Chem. Mater.* **1993**, 5, 412.
- 5 R. Xu, H. C. Zeng, *J. Phys. Chem. B* **2003**, 107, 926.
- 6 J. Feng, H. C. Zeng, *Chem. Mater.* **2003**, 15, 2829.
- 7 M. Ando, T. Kobayashi, S. Iijima, M. Haruta, *J. Mater. Chem.* **1997**, 7, 1779.
- 8 L. Cao, M. Lu, H.-L. Li, *J. Electrochem. Soc.* **2005**, 152, A871.
- 9 X. Wang, X. Chen, L. Gao, H. Zheng, Z. Zhang, Y. Qian, *J. Phys. Chem. B* **2004**, 108, 16401.
- 10 W. Y. Li, L. N. Xu, J. Chen, *Adv. Funct. Mater.* **2005**, 15, 851.
- 11 H. Y. Guan, C. L. Shao, S. B. Wen, *Mater. Chem. Phys.* **2003**, 82, 1002.
- 12 J. Feng, H. C. Zeng, *Chem. Mater.* **2003**, 15, 2829.
- 13 T. He, D. Chen, X. Jiao, Y. Xu, Y. Gu, *Langmuir* **2004**, 20, 8404.
- 14 R. M. Wang, C. M. Liu, H. Z. Zhang, C. P. Chen, L. Guo, H. B. Xu, S. H. Yang, *Appl. Phys. Lett.* **2004**, 85, 2080.
- 15 Z. Gui, J. Liu, Z. Wang, L. Song, Y. Hu, W. Fan, D. Chen, *J. Phys. Chem. B* **2005**, 109, 1113.
- 16 Z. Wang, X. Chen, M. Zhang, Y. Qian, *Solid State Sci.* **2005**, 7, 13.
- 17 W. Zhang, D. Ma, J. Liu, L. Kong, W. Yu, Y. Qian, *Carbon* **2004**, 42, 2341.
- 18 Y. J. Zhu, S. H. Deng, S. P. Yi, S. Zhong, Y. L. Chen, Y. Y. He, H. Y. Zhang, *J. Inorg. Mater.* **2003**, 18, 1267.